An X-ray and Neutron Diffraction Structure Analysis of a Triply-bridged Binuclear Iridium Complex, $[[(C_5(CH_3)_5Ir)_2(\mu\text{-}H)_3]^+[ClO_4]^-\cdot 2C_6H_6]$

RAYMOND C. STEVENS, MALCOLM R. MCLEAN, THERESA WEN, JOHN D. CARPENTER, ROBERT BAU*
Department of Chemistry, University of Southern California, Los Angeles, CA 90089-0744 (U.S.A.)
and THOMAS F. KOETZLE*
Chemistry Department, Brookhaven National Laboratory, Upton, NY 11973-5000 (U.S.A.)

(Received October 31, 1988; revised February 9, 1989)

Abstract

The structure of $[[(C_5(CH_3)_5Ir)_2(\mu\text{-}H)_3]^+[ClO_4]^-\cdot 2C_6H_6]$ has been studied with X-ray and neutron diffraction techniques at room temperature and 21 K, respectively. Crystal data from the X-ray diffraction analysis of the title compound at room temperature: space group *Pnnm*; a = 13.358(4), b = 14.083(4), c = 8.846(3) Å; V = 1664.3(9) Å^3; Z = 2. Final agreement factors are $R(F)$ = 0.026 and $R(wF)$ = 0.034 for 1007 independent X-ray reflections with $I > 3\sigma(I)$ and 130 parameters varied. Crystal data for the neutron diffraction analysis at 21 K: space group $P2_12_12$; a = 13.261(3), b = 13.625(3), c = 8.612(2) Å; V = 1556.0(8) Å^3; Z = 2. Final agreement factors are $R(F)$ = 0.038 and $R(wF)$ = 0.042 for 2315 independent neutron reflections and 393 parameters varied. The neutron diffraction study represents the first accurate structure determination of a symmetric dimer with a metal–metal bond bridged by three hydride ligands. Average molecular parameters are: Ir–H = 1.78(1), Ir–Ir = 2.465(3), H···H = 2.22(2) Å, Ir–H–Ir = 87.8(4)°, H–Ir–H = 77.2(7)°, H–H–H = 60.0(7)°.

Introduction

Over the past years, our group has been studying the structures of metal complexes of the type M–$(H)_n$–M by neutron diffraction, in order to obtain basic structural information on hydrogen bridged metal–metal bonds. Thus far, symmetric bridged hydrides with n = 1,2,4 have been accurately characterized [1–5] by ourselves and others; but the analysis of a compound having three hydrogen bridges $[(C_5(CH_3)_5Ir)_2(\mu\text{-}H)_3]^+[BF_4]^-$, ($\mathbf{1}^+[BF_4]^-$), was complicated by the presence of disorder, and was of relatively low precision [6, 7]. In the present paper we report the neutron diffraction study of $[[C_5(CH_3)_5Ir)_2(\mu\text{-}H)_3]^+[ClO_4]^-\cdot 2C_6H_6]$, which provides more precise parameters for the M–$(\mu\text{-}H)_3$–M linkage, thereby completing the sequence of measurements on symmetrical M–$(\mu\text{-}H)_3$–M (n = 1,2,3,4)**. From a catalytic viewpoint, $\mathbf{1}^+$ is of additional interest because it is the final hydrogenation product of the olefin hydrogenation and isomerization catalyst **2** [9], which also is a bridged hydride species. $\mathbf{1}^+$ is formed starting from $[C_5(CH_3)_5IrCl_2]_2$ by the stepwise replacement of bridging halides with hydrides which are themselves derived from the heterolytic splitting of hydrogen gas.

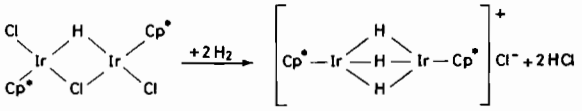

2 $\mathbf{1}^+$

Cp* = $C_5(CH_3)_5$

As mentioned above, the structure of $\mathbf{1}^+$ had previously been studied by us in a neutron diffraction analysis at 20 K on a plate-like crystal of $\mathbf{1}^+[BF_4]^-$ [6, 7]. Unfortunately, that earlier analysis was somewhat unsatisfactory, resulting in an incompletely refined structure ($R(F)$ = 0.18), due to the poor quality of the crystals and the disorder of the hydride ligands (which had thermal parameters corresponding to unusually elongated cigar-shaped ellipsoids). These factors prevented the structure analysis from attaining the desired precision, and therefore the study was abandoned at that stage, remaining unresolved and only partial results were published [6]. It was decided to reexamine $\mathbf{1}^+$, and hopefully to grow a large crystal of better quality which would be more suitable for neutron diffraction. Preliminary experimentation had shown some promise with the $[PF_6]^-$ salt (J.C.), and an X-ray structural analysis

*Authors to whom correspondence should be addressed.

**It should be pointed out, however, that a neutron diffraction study of an asymmetric M–$(\mu\text{-}H)_3$–M compound, $[Et_4N]^+[(triphos)Re_2(\mu\text{-}H)_3(H)_6]^-\cdot CH_3CN$, has been reported [8].

0020-1693/89/$3.50

was carried out on this second derivative (T.W.). However, the $[PF_6]^-$ salt tended to grow as thin plates, still too small for a neutron analysis. In the present paper, we report that larger, high quality crystals can be obtained using the $[ClO_4]^-$ anion, and ultimately it was this third derivative which produced the crystal used in the neutron study reported here.

Experimental

Materials

$IrCl_3 \cdot 3H_2O$ was purchased from Strem and used as received; H_2 gas (ultra-high purity, >99.999%) and argon gas (pre-purified, >99.998%) were purchased from M.G. Industries. HCl gas (reagent grade) was purchased from Speciality Products and Equipment. All solvents were purchased from J. T. Baker and used as received, unless otherwise noted. The Na^+ salts of $[BF_4]^-$, $[ClO_4]^-$ and $[B(Ph)_4]^-$ were purchased from Aldrich and used as received. Hexamethyldewarbenzene (HMBD-Aldrich) was stored in a freezer in sealed vials until required, and then opened and used immediately. Methanol was refluxed with, and then distilled from calcium hydride, under an atmosphere of argon. The synthetic steps are modification of published procedures [9, 10].

Proton NMR spectra were recorded in $CDCl_3$ solutions on a Jeol FX-90Q instrument at 90 MHz field, using residual $CHCl_3$ in the deuterated solvent as an internal standard. Although the final product is not particularily air-sensitive, some of the synthetic steps involved the handling of air sensitive precursors. Standard Schlenkware and vacuum line techniques were utilized for such steps, as noted in the following text.

$[(C_5(CH_3)_5Ir)_2(\mu\text{-}H)_3]^+[ClO_4]^-$

This derivative was produced by dissolving the very soluble chloride salt in a minimum amount of distilled water and filtering the solution into a slight excess of a concentrated aqueous solution of Na^+-$[ClO_4]^-$. Precipitation ensued immediately, and the resulting perchlorate salt was collected by filtration (the filtrate was colorless), and washed with a minimum amount of cold water, and then dried exhaustively under vacuum. IR (KBr disk): 1100 cm^{-1} ν(Cl–O)(s). [**Warning**: perchlorate salts are notoriously shock-sensitive and prone to detonate. Although the explosive properties of this derivative were never investigated, it is recommended that no more than 25 mg be isolated (i.e., in the dry state) at any one time.]

Crystal Growth

No precautions for air sensitivity were needed in the crystal growth procedures. A portion of perchlorate was dissolved in a minimum amount (5 ml) of dry (stored over Linde type 4(A) molecular sieves) CH_2Cl_2, and then benzene was slowly added to this solution until it became turbid, followed by a slow dropwise addition of CH_2Cl_2 until the precipitate redissolved (total volume approximately 8 ml). The solution was then filtered into a suitable vapor diffusion crystallization setup with an excess volume (10 ml) of pentane as the precipitant and placed in the freezer (−22 °C) for a week. This technique slows crystal growth and thus enhances the chance of obtaining one large, good-quality crystal, as opposed to many small ones. Such a technique routinely resulted in the deposition of large, lemon–yellow, transparent crystals of $\mathbf{1}^+[ClO_4]^-$.

X-ray Diffraction

A preliminary room temperature X-ray diffraction structure analysis on a small yellow crystal of $[[(C_5(CH_3)_5Ir)_2(\mu\text{-}H)_3]^+[ClO_4]^- \cdot 2C_6H_6]$ revealed the expected $(C_5(CH_3)_5Ir)_2(\mu\text{-}H)_3$ cationic core (no hydrogen atoms were located in the X-ray study), one $[ClO_4]^-$ counter-ion, and the two benzene molecules of solvation. The presence of benzene solvate was anticipated, from previous experience in handling the crystals, which had shown a strong tendency to desolvation. As a result, the crystal used for the intensity measurements was mounted in air on a glass fiber with Super Glue, and then rapidly coated with more Super Glue to minimize decomposition via desolvation. This technique proved successful, as evidenced by the fact that the faces of the crystal could still clearly be seen through the translucent adhesive during the crystal centering operations. Data were collected on a four-circle Nicolet/Syntex $P2_1$ automated diffractometer employing Mo Kα radiation. The unit cell constants and orientation matrix were obtained from 15 centered reflections ($20° < 2\theta < 25°$). The unit cell parameters and other relevant data are presented in Table 1. Monitoring three check reflections [(6 4 0) (5 0 3) (6 3 1)] at 50-reflection intervals revealed no significant variation in intensity. The raw data were reduced to yield integrated intensities of 1007 independent reflections satisfying the criterion $I > 3\sigma(I)$. The intensities were corrected for Lorentz, polarization and absorption effects. The space group was determined to be *Pnnm*, consistent with the extinctions of $0kl$, $k + l = 2n$; $h0l$, $h + l = 2n$. The coordinates of the unique iridium atom were obtained from a Patterson map, and the other non-hydrogen atoms were located from successive difference-Fourier maps. The cation has crystallographic $2/m$ symmetry. All atoms were refined anisotropically. SHELX76 was used in the structure solution [11]. See also 'Supplementary Material'.

TABLE 1. Summary of crystal data and refinement results for $[[(C_5(CH_3)_5Ir)_2(\mu\text{-}H)_3]^+[ClO_4]^-\cdot 2C_6H_6]$

	X-ray (298 K)	Neutron (21 K)
Space group	*Pnnm*	$P2_12_12$
a (Å)	13.358(4)	13.261(3)
b (Å)	14.083(4)	13.625(3)
c (Å)	8.846(3)	8.612(2)
V (Å^3)	1664.3(9)	1556.0(8)
Density (calc.) (g cm^{-3})	1.667	1.783
Crystal dimensions (mm)	0.6 × 0.3 × 0.5	3.0 × 1.5 × 1.0
Wavelength (Å)	0.71069	1.15882(7)
Absorption coefficient (μ) (cm^{-1})	159.91	2.76
Sin θ/λ limit (Å^{-1})	0.5385	0.6846
Total no. reflections measured	1374	4060
No. independent reflections	1320	2315
No. reflections used in structural analysis	1007 [$I > 3\sigma(I)$]	2315
No. variable parameters	130	393
Final agreement factors		
$R(F)$	0.026	0.038
$R(wF)$	0.034	0.042
Goodness of fit (F)		1.342
$R(F^2)$		0.058
$R(wF^2)$		0.067
Goodness of fit (F^2)		1.358

Neutron Diffraction

Neutron diffraction data were collected at the Brookhaven High Flux Beam Reactor [12, 13] at 21 K on a large, transparent, lemon–yellow crystal which had been mounted on an aluminum pin approximately along the a^* direction and placed in a specially adapted closed-cycle helium refrigerator [14]. Monitoring of one reflection (0 6 0) during cooling (298 to 21 K) revealed no significant variation in intensity. However, the crystal was found to undergo a reversible, non-destructive phase transition associated with ordering of the $[ClO_4]^-$ counter-ions, with a change of space group from *Pnnm* at room temperature to $P2_12_12$ at the temperature of neutron data collection (21 K). Actually, this phase transition was not detected at first, since no change in the intensity of the monitored reflection (0 6 0) was discernible. It was only after difficulties were encountered during the structure analysis that it was suspected that a change in space group may have taken place. To test this hypothesis, the cooling experiment was repeated, on the same crystal used in the data collection, and five reflections were monitored in place of the previous one. Closely following the variation in intensity of these five reflections (allowed in $P2_12_12$ and having strong intensity at 21 K but extinct in *Pnnm*) with temperature revealed the presence of the reversible phase transition. All five reflections rapidly diminished in intensity as the temperature increased towards the transition point, and disappeared completely at the transition temperature. The same situation occurred in reverse upon recooling through the transition. This left no doubt that we were observing a non-destructive, reversible phase change; the transition temperature was determined to be 225(1) K.

The space group was determined to be $P2_12_12$ in the low temperature neutron case, consistent with the extinctions of $h00$, $h = 2n$ and $0k0$, $k = 2n$. In this space group, the anion lies across the two-fold axis. The non-hydrogen atoms were located with MULTAN [15], and the hydrogen atoms were then located from successive difference-Fourier maps. Several cycles of refinement of the non-bridging atoms, in which all positional and anisotropic thermal parameters were varied, were performed by means of differential synthesis [16], until all non-bridging hydrogen atoms had been located. Full-matrix least-squares refinement [17] was then carried out, yielding an $R(F)$ value of 0.060. The bridging hydrogen atoms were located from a difference-Fourier map (see Fig. 2) and found to be disordered about the two-fold axis. The disordered model (with six half-hydrogens) was refined with full-matrix least-squares until convergence was obtained at an $R(F)$ value of 0.038. Due to the disorder of the bridging hydrogens, the thermal parameters of these atoms were refined isotropically in the final cycles. An isotropic type I, extinction correction with Lorentzian mosiac was applied [18]. The quantity minimized in the least-squares refinement was $\Sigma w(F_{obs}^2 - F_{calc}^2)^2$ with $w = (\sigma_{count}^2 + 0.02F_o^2)^2)^{-1}$. A final difference map was essentially featureless. Atomic positional and thermal parameters are given in Tables 2 and 3 respectively. See also 'Supplementary Material'.

Neutron scattering lengths were taken from a compilation of Koester [19]. Computer programs employed include MULTAN [15] (direct methods), DIFSYN [16] (differential synthesis program), a modified version of UPALS [17] (full-matrix least-squares program), the absorption correction procedure of Coppens *et al.* [20], Johnson's ORTEP2 [21] and locally written programs.

Results and Discussion

Crystals of the title complex diffracted neutrons well, and refinement of the structure proceeded smoothly, once the change in space group on cooling was recognized. Aside from the ordering of the $[ClO_4]^-$ ions, no substantial difference in the crystal packing was observed between the room temperature

TABLE 2. Atomic coordinates for $[[(C_5(CH_3)_5Ir)_2(\mu\text{-}H)_3]^+\cdot[ClO_4]^-\cdot 2C_6H_6]$ from the neutron diffraction study at 21 K

Atom	Occupancy	x	y	z
Ir1	1.000000	0.5900(1)	0.0225(1)	0.2140(1)
HB1	0.500000	0.5117(9)	−0.036(1)	0.076(1)
HB2	0.500000	0.5161(9)	−0.057(1)	0.330(2)
HB3	0.500000	0.4766(9)	−0.9103(9)	0.229(2)
Centroid[a]		0.5000	0.0000	0.2115
C1	1.000000	0.7409(2)	−0.0233(1)	0.2839(2)
C2	1.000000	0.7144(2)	0.0661(1)	0.3630(2)
C3	1.000000	0.6979(2)	0.1407(1)	0.2473(2)
C4	1.000000	0.7142(2)	0.0976(1)	0.0967(2)
C5	1.000000	0.7412(2)	−0.0038(2)	0.1195(2)
Centroid[b]		0.7217	0.0555	0.2221
C11	1.000000	0.7685(2)	−0.1186(2)	0.3580(2)
C21	1.000000	0.7104(2)	0.0807(2)	0.5354(2)
C31	1.000000	0.6726(2)	0.2461(2)	0.2782(2)
C41	1.000000	0.7105(2)	0.1490(2)	−0.0563(2)
C51	1.000000	0.7712(2)	−0.0742(2)	−0.0051(2)
H11A	1.000000	0.7509(5)	0.3194(4)	−0.2844(7)
H11C	1.000000	0.6510(4)	0.3784(5)	−0.3814(9)
H21A	1.000000	0.7842(4)	0.1008(5)	−0.4220(6)
H21B	1.000000	0.6896(6)	0.0121(4)	−0.4046(6)
H21C	1.000000	0.6566(5)	0.1376(4)	−0.4328(6)
H31A	1.000000	0.7430(4)	0.2886(4)	−0.7181(8)
H31B	1.000000	0.6237(5)	0.2773(4)	0.1902(6)
H31C	1.000000	0.6354(4)	0.2554(4)	−0.6110(6)
H41A	1.000000	0.6631(5)	0.2134(4)	−0.0522(6)
H41B	1.000000	0.6797(5)	0.1006(4)	−0.1459(6)
H41C	1.000000	0.7867(5)	0.1691(4)	−0.0910(6)
H51A	1.000000	0.7523(5)	0.4500(4)	0.1192(6)
H51B	1.000000	0.7621(5)	0.3533(4)	−0.0136(7)
H51C	1.000000	0.6470(4)	0.4186(4)	0.0070(8)
Cl1	0.500000	0.000000	0.000000	−0.2688(2)
O1	1.000000	0.9182(2)	−0.0336(2)	−0.3636(3)
O2	1.000000	0.9661(3)	0.0797(4)	−0.1746(6)
CS1	1.000000	0.9534(2)	0.1641(2)	0.1819(3)
CS2	1.000000	0.9507(2)	0.1553(2)	0.3436(3)
CS3	1.000000	0.9501(2)	0.2379(2)	0.4381(3)
CS4	1.000000	0.9528(2)	0.3304(2)	0.3697(4)
CS5	1.000000	0.9554(2)	0.3401(2)	0.2079(4)
CS6	1.000000	0.9560(2)	0.2571(2)	0.1150(3)
HS1	1.000000	0.9543(6)	0.0985(5)	0.1085(7)
HS2	1.000000	0.9496(5)	0.0816(6)	−0.6034(7)
HS3	1.000000	0.9485(6)	0.2284(5)	−0.4365(6)
HS4	1.000000	0.9545(6)	0.3962(5)	−0.5575(9)
HS5	1.000000	0.9572(6)	0.4137(5)	0.156(1)
HS6	1.000000	0.9586(6)	0.2649(6)	−0.0106(7)

[a]Bridging hydride centroid. [b]Ring centroid.

TABLE 3. Anisotropic temperature factors for $[[(C_5(CH_3)_5Ir)_2(\mu\text{-}H)_3]^+[ClO_4]^-\cdot 2C_6H_6]$ from the neutron diffraction study at 21 K

Atom	β_{11}	β_{22}	β_{33}	β_{12}	β_{13}	β_{23}
Ir1	0.0004(1)	0.0005(1)	0.0004(1)	0.0000(1)	0.0000(1)	0.0001(1)
HB1	0.0013(6)	0.009(1)	0.007(1)	−0.0006(7)	−0.0003(8)	−0.005(1)
HB2	0.0015(7)	0.007(1)	0.014(2)	−0.0016(7)	−0.0021(1)	0.008(1)
HB3	0.0029(7)	0.0021(5)	0.019(2)	−0.0002(5)	0.001(1)	−0.001(1)
C1	0.0005(1)	0.0007(1)	0.0016(2)	−0.0000(1)	0.0000(1)	0.0001(1)
C2	0.0003(1)	0.0009(1)	0.0014(2)	0.0000(1)	−0.0000(1)	−0.0001(1)
C3	0.0003(1)	0.0006(1)	0.0017(2)	−0.0001(1)	0.0003(1)	0.0000(1)
C4	0.0004(1)	0.0004(1)	0.0013(2)	0.0000(1)	0.0000(1)	0.0000(1)
C5	0.0004(1)	0.0007(1)	0.0015(2)	−0.0001(1)	0.0003(1)	−0.0002(1)
C11	0.0009(1)	0.0006(1)	0.0027(2)	0.0002(1)	0.0001(1)	0.0004(1)
C21	0.0006(1)	0.0013(1)	0.0016(2)	0.0000(1)	−0.0000(1)	−0.0001(1)
C31	0.0011(1)	0.0004(1)	0.0024(2)	−0.0002(1)	0.0003(1)	−0.0002(1)
C41	0.0012(1)	0.0008(1)	0.0011(2)	−0.0000(1)	0.0001(1)	0.0001(1)
C51	0.0011(1)	0.0010(1)	0.0017(1)	0.0001(1)	0.0002(1)	−0.0005(1)
H11A	0.0057(4)	0.0015(2)	0.0090(7)	0.0002(3)	−0.0020(5)	0.0002(3)
H11B	0.0048(4)	0.0036(3)	0.0075(7)	−0.0010(3)	0.0024(5)	−0.0025(4)
H11C	0.0019(3)	0.0037(3)	0.015(1)	−0.0001(2)	−0.0016(5)	−0.0024(5)
H21A	0.0015(3)	0.0067(4)	0.0057(6)	−0.0011(3)	−0.0007(4)	−0.0017(4)
H21B	0.0070(5)	0.0024(2)	0.0046(5)	−0.0006(3)	0.0008(4)	0.0006(3)
H21C	0.0041(4)	0.0030(3)	0.0059(7)	0.0016(3)	−0.0004(4)	−0.0010(4)
H31A	0.0025(3)	0.0019(2)	0.0131(8)	−0.0008(2)	0.0003(5)	−0.0010(4)
H31B	0.0042(4)	0.0021(2)	0.0066(6)	0.0007(2)	−0.0019(4)	0.0006(3)
H31C	0.0035(3)	0.0028(2)	0.0056(6)	0.0008(3)	0.0021(4)	−0.0007(4)
H41A	0.0043(4)	0.0019(2)	0.0066(6)	0.0013(3)	0.0005(4)	0.0011(3)
H41B	0.0052(4)	0.0031(3)	0.0040(6)	−0.0008(3)	−0.0021(4)	−0.0005(4)

(continued)

TABLE 3. *(continued)*

Atom	β_{11}	β_{22}	β_{33}	β_{12}	β_{13}	β_{23}
H41C	0.0024(3)	0.0049(3)	0.0064(6)	−0.0008(3)	0.0009(3)	0.0026(4)
H51A	0.0057(5)	0.0031(3)	0.0040(5)	−0.0017(3)	−0.0007(4)	−0.0000(3)
H51B	0.0039(4)	0.0014(2)	0.0106(8)	0.0005(2)	0.0027(4)	0.0013(3)
H51C	0.0012(3)	0.0039(3)	0.0131(9)	−0.0003(3)	0.0018(4)	0.0036(5)
Cl1	0.0005(1)	0.0014(1)	0.0015(2)	−0.0004(1)	0.000000	0.000000
O1	0.0011(1)	0.0013(1)	0.0031(2)	−0.0004(1)	−0.0007(1)	0.0004(2)
O2	0.0024(2)	0.0070(3)	0.0177(7)	−0.0031(2)	0.0052(3)	−0.0100(4)
CS1	0.0010(1)	0.0023(1)	0.0041(3)	−0.0002(1)	−0.0002(2)	0.0010(2)
CS2	0.0008(1)	0.0020(1)	0.0036(3)	−0.0003(1)	−0.0000(2)	0.0010(2)
CS3	0.0010(1)	0.0021(1)	0.0052(3)	−0.0002(1)	−0.0001(2)	0.0006(2)
CS4	0.0008(1)	0.0017(1)	0.0102(4)	−0.0000(1)	−0.0002(2)	0.0006(2)
CS5	0.0010(1)	0.0021(1)	0.0109(4)	−0.0003(1)	−0.0008(2)	0.0030(2)
CS6	0.0012(1)	0.0029(1)	0.0060(3)	−0.0004(1)	−0.0002(2)	0.0024(2)
HS1	0.0037(4)	0.0045(4)	0.0090(7)	−0.0006(3)	0.0003(5)	−0.0017(5)
HS2	0.0038(4)	0.0025(3)	0.0092(7)	0.0000(3)	−0.0004(5)	0.0015(4)
HS3	0.0055(4)	0.0048(4)	0.0058(7)	−0.0000(4)	0.0003(5)	−0.0011(4)
HS4	0.0036(4)	0.0033(3)	0.017(1)	−0.0003(3)	0.0009(6)	−0.0014(5)
HS5	0.0036(4)	0.0035(3)	0.022(1)	−0.0003(3)	−0.0012(6)	0.0055(6)
HS6	0.0039(4)	0.0073(5)	0.0065(7)	−0.0006(4)	−0.0003(4)	0.0035(5)

The form of the anisotropic thermal factor is: $\exp[-(h^2\beta_{11} + k^2\beta_{22} + l^2\beta_{33} + 2hk\beta_{12} + 2hl\beta_{13} + 2kl\beta_{23})]$.

and low-temperature phases. Surprisingly, however, an examination of ORTEP plots revealed the same cigar-shaped hydride thermal ellipsoids (Fig. 1) which had been observed in the previously examined $[BF_4]^-$ derivative [6, 7]. This occurred in spite of the much improved agreement [$R(F) = 0.038$ for this study versus 0.18 for the previous one] and the fact that the present data set had been collected at the low temperature of 21 K. In the model illustrated in Fig. 1, the hydride ligands have been refined anisotropically, and their ellipsoids can be seen to elongated in the plane normal to the Ir–Ir bond.

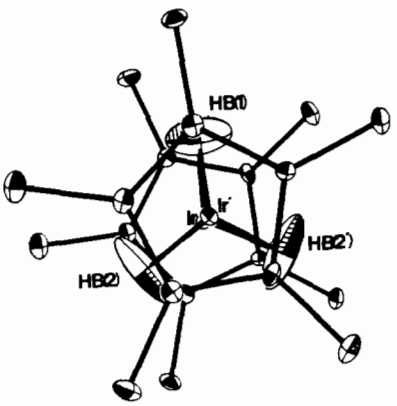

Fig. 1. ORTEP view down the Ir–Ir bond illustrating the 'cigar shaped' thermal ellipsoids resulting from treating each pair of half-occupied bridging hydrogens as a single site. In this model, HB(1) lies on the C_2 axis. Methyl hydrogens have been removed for clarity. Thermal ellipsoids are drawn at the 75% probability level [21].

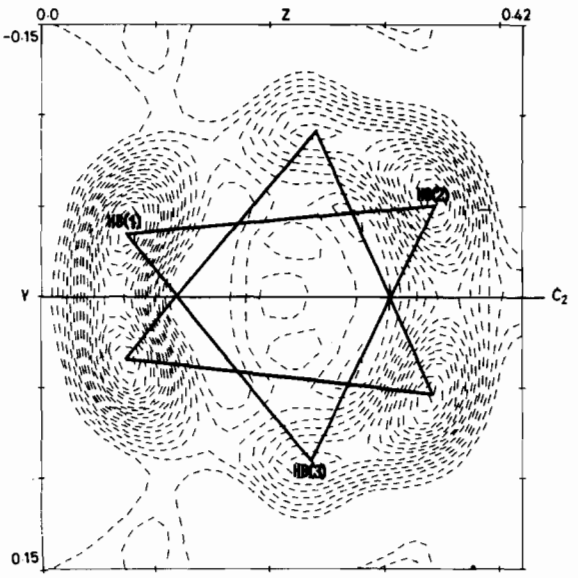

Fig. 2. Difference Fourier section (x = 1/2) in the plane normal to the Ir–Ir bond, with the two-fold axis horizontal and showing the six disordered bridging hydrogen peaks [17].

Further investigation into this phenomenon uncovered disorder in the structure, as evidenced by a six-peak, pseudohexagonal arrangement of the nuclear density in the plane of the hydrogens (Fig. 2). For clarity, the two sets of three half-hydrogens related by the two-fold axis have been linked to form two equilateral triangles. This disorder involving

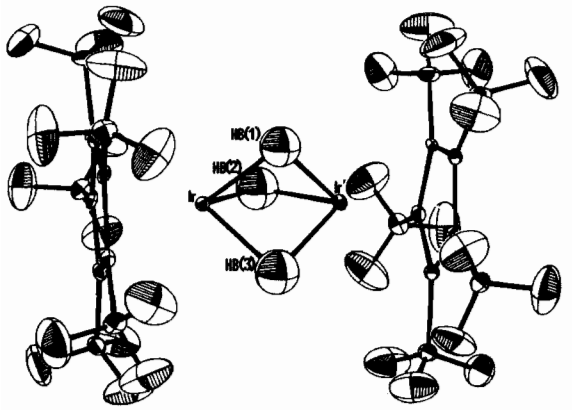

Fig. 3. ORTEP view normal to the Ir–Ir bond [21].

the bridging hydride ligands then was taken into account, and the refinement was continued with the six half-occupied hydrogens (refined isotropically), resulting in the final structure model shown in Fig. 3. (It should be pointed out that this Figure shows only one of the two sets of three half-occupied hydrogens.) The R factor remained unchanged (0.038) with the six half-hydrogen isotropic model.

Bond distances and angles involving the bridging hydrides are given in Table 4. The M–H bond distances are normal, with a mean value of 1.78(1) Å. This distance can be compared with mean values in, for example, the quadruply-bridged Re–(μ-H)$_4$–Re dimer [5], [(PEt$_2$Ph)$_2$]$_2$(μ-H)$_4$(H)$_4$ with Re–H = 1.878(8) Å; and the two doubly-bridged M–(μ-

TABLE 4. Bridging hydride bond distances (Å) and angles (°) in the $[(C_5(CH_3)_5Ir)_2(\mu\text{-}H)_3]^+$ cation, from the neutron diffraction study at 21 K

Ir–Ir	2.465(3)		
Ir–HB1	1.76(1)	Ir–Centroid[a]	1.23(1)
Ir–HB1	1.81(1)	H1–Centroid[a]	1.27(2)
Ir–HB2	1.77(2)	H2–Centroid[a]	1.30(2)
Ir–HB2′	1.79(1)	H3–Centroid[a]	1.27(2)
Ir–HB3	1.76(1)	H1′–Centroid[a]	1.27(2)
Ir–HB3′	1.77(1)	H2′–Centroid[a]	1.30(2)
Mean Ir–H	1.78(1)	H3′–Centroid[a]	1.27(2)
		Mean H–Centroid[a]	1.28(2)
HB1–HB2	2.20(2)		
HB1–HB3	2.20(2)	H1–Centroid[a]–Ir	90(1)
HB2–HB3	2.24(2)	H2–Centroid[a]–Ir	89(1)
HB1–HB1′	1.02(3)	H3–Centroid[a]–Ir	90(1)
HB1–HB3′	1.51(2)	H1′–Centroid[a]–Ir	92(1)
HB2–HB2	1.61(3)	H2′–Centroid[a]–Ir	90(1)
HB2–HB3′	0.98(2)	H3′–Centroid[a]–Ir	90(1)
		Mean H–Centroid[a]–Ir	90(1)
HB1–Ir–HB2	77.2(6)		
HB1–Ir–HB3	77.2(7)		
HB2–Ir–HB3	78.7(7)	Centroid[a]–Centroid[b]	3.04(1)
HB1′–Ir–HB2′	75.7(6)	Centroid[a]–Ir–Centroid[b]	178.8(6)
HB1′–Ir–HB3′	76.1(7)	Ir–Centroid[a]–Ir	178(1)
HB2′–Ir–HB3′	78.1(7)		
Mean H–Ir–H	77.2(7)		
HB1–HB2–HB3	59.4(7)	Ir–HB1–Ir′	87.3(4)
HB2–HB1–HB3	61.1(7)	Ir–HB2–Ir′	87.8(5)
HB1–HB3–HB2	59.5(6)	Ir–BH3–Ir′	88.4(4)
Mean H–H–H	60.0(7)	Mean Ir–H–Ir′	87.8(4)
HB1–Ir–Centroid[b]	135.0(4)		
HB2–Ir–Centroid[b]	131.9(4)		
HB3–Ir–Centroid[b]	133.9(4)		
HB1′–Ir–Centroid[b]	136.4(4)		
HB2′–Ir–Centroid[b]	132.5(5)		
HB3′–Ir–Centroid[b]	134.0(4)		
Mean H–Ir–Centroid[b]	134.0(4)		

The prime (′) notation is used to denote the symmetry (two-fold) related sites. [a]Bridging hydride centroid. [b]C_5Me_5 ring centroid.

TABLE 5. Bond distances (Å) and angles (°) for $[(C_5(CH_3)_5Ir)_2(\mu\text{-}H)_3]^+[ClO_4]^-\cdot 2C_6H_6$

	X-ray	Neutron		X-ray	Neutron
$C_5(CH_3)_5$ Ring			$[ClO_4]^-$		
C1–C2	1.41(2)	1.440(3)	Cl–O1	1.41(3)	1.433(3)
C2–C3	1.43(1)	1.439(3)	Cl–O1′	1.40(4)	1.433(3)
C3–C4	1.43(1)	1.440(3)	Cl–O2	1.38(3)	1.429(4)
C4–C5	1.41(2)	1.441(3)	Cl–O2′	1.47(3)	1.429(4)
C1–C5	1.47(3)	1.440(3)	Mean Cl–O	1.42(3)	1.431(4)
Mean C–C	1.43(2)	1.440(3)			
			O1–Cl–O1′	109(2)	110.6(2)
C1–C2–C3	109(1)	107.9(2)	O1–Cl–O2	110(2)	109.1(2)
C2–C3–C4	107(1)	108.2(2)	O1–Cl–O2′	116(2)	108.6(2)
C3–C4–C5	109(1)	107.8(2)	O2–Cl–O2′	105(2)	110.8(5)
C4–C5–C1	107(1)	108.1(2)	O2–Cl–O1′	110(2)	108.6(2)
C5–C1–C2	107(1)	108.0(2)	O2′–Cl–O1′	106(2)	109.1(2)
Mean C–C–C	108(1)	108.0(2)	Mean O–Cl–O	109(2)	109.5(3)
			C_6H_6		
Ir–C1	2.18(1)	2.181(2)			
Ir–C2	2.18(1)	2.173(2)	CS1–CS2	1.44(2)	1.392(4)
Ir–C3	2.17(1)	2.173(2)	CS2–CS3	1.25(2)	1.398(3)
Ir–C4	2.17(1)	2.186(2)	CS3–CS4	1.29(2)	1.400(4)
Ir–C5	2.17(1)	2.192(2)	CS4–CS5	1.46(2)	1.392(4)
Mean Ir–C	2.18(1)	2.181(2)	CS5–CS6	1.29(2)	1.390(4)
Ir–Centroid	1.80(1)	1.789(2)	CS6–CS1	1.25(2)	1.398(3)
			Mean C–C	1.33(2)	1.395(4)
C1–C11	1.49(2)	1.492(3)			
C2–C21	1.50(2)	1.499(3)	CS1–CS2–CS3	118(1)	120.3(2)
C3–C31	1.47(2)	1.499(3)	CS2–CS3–CS4	126(1)	119.8(2)
C4–C41	1.50(2)	1.494(3)	CS3–CS4–CS5	116(1)	120.5(3)
C5–C51	1.49(2)	1.494(3)	CS4–CS5–CS6	116(1)	119.1(2)
Mean C–C	1.49(2)	1.496(3)	CS5–CS6–CS1	126(1)	120.9(2)
			CS6–CS1–CS2	118(1)	119.4(3)
C2–C1–C11	127(1)	126.4(2)	Mean C–C–C	120(1)	120.0(2)
C5–C1–C11	126(1)	125.5(2)			
C1–C2–C21	126(1)	125.9(2)	CS1–HS1	1.095(7)	
C3–C2–C21	125(1)	126.1(2)	CS2–HS2	1.088(6)	
C2–C3–C31	126(1)	126.0(2)	CS3–HS3	1.097(7)	
C4–C3–C31	126(1)	125.7(2)	CS4–HS4	1.094(8)	
C3–C4–C41	126(1)	126.8(2)	CS5–HS5	1.088(6)	
C5–C4–C41	125(1)	125.3(2)	CS6–HS6	1.103(6)	
C4–C5–C51	127(1)	126.0(2)	Mean C–H	1.094(7)	
C1–C5–C51	126(1)	125.8(2)			
Mean C–C–C	126(1)	126.0(2)	CS2–CS1–HS1	120.2(4)	
			CS6–CS1–HS1	120.3(4)	
			CS1–CS2–HS2	120.1(5)	
			CS3–CS2–HS2	119.6(5)	
			CS2–CS3–HS3	120.8(5)	
			CS4–CS3–HS3	119.3(5)	
			CS3–CS4–HS4	119.5(5)	
			CS5–CS4–HS4	120.0(5)	
			CS4–CS5–HS5	119.0(4)	
			CS6–CS5–HS5	121.9(4)	
			CS5–CS6–HS6	119.4(4)	
			CS1–CS6–HS6	119.7(4)	
			Mean C–C–H	120.0(4)	
Methyl hydrogens from $C_5(CH_3)_5$ for neutron case					
C11–H11A	1.086(6)	C11–H11B	1.087(6)	C11–H11C	1.097(6)
C21–H21A	1.080(6)	C21–H21B	1.088(6)	C21–H21C	1.103(6)
C31–H31A	1.081(5)	C31–H31B	1.084(6)	C31–H31C	1.098(6)
C41–H41A	1.079(6)	C41–H41B	1.090(6)	C41–H41C	1.094(6)
C51–H51A	1.082(5)	C51–H51B	1.089(6)	C51–H51C	1.094(6)
Mean C–H	1.089(6)				

(continued)

TABLE 5. *(continued)*

C1–C11–H11A	111.6(4)	C1–C11–H11B	111.5(4)	C1–C11–H11C	110.6(4)
C2–C21–H21A	109.7(4)	C2–C21–H21B	111.1(3)	C2–C21–C21C	111.5(4)
C3–C31–H31A	108.7(3)	C3–C31–H31B	112.7(3)	C3–C31–H31C	111.8(4)
C4–C41–H41A	111.8(3)	C4–C41–H41B	110.6(3)	C4–C41–H41C	109.2(4)
C5–C51–H51A	112.3(4)	C5–C51–H51B	111.6(4)	C5–H51–H51C	109.5(4)
Mean C–C–H	110.9(4)				
H11A–C11–H11B	108.2(6)	H11A–C11–H11C	106.9(5)	H11B–C11–H11C	107.9(6)
H21A–C21–H21B	109.1(5)	H21A–C21–H21C	106.4(6)	H21B–C21–H21C	108.8(6)
H31A–C31–H31B	107.4(5)	H31A–C31–H31C	107.5(5)	H31B–C31–H31C	108.7(5)
H41A–C41–H41B	107.3(5)	H41A–C41–H41C	110.1(5)	H41B–C41–H41C	107.7(5)
H51A–C51–H51B	107.0(5)	H51A–C51–H51C	107.5(5)	H51B–C51–H51C	108.8(5)
Mean H–H–H	108.0(5)				

$H)_2$–M complexes $H_2Os_3(CO)_{10}$ with Os–H = 1.850(5) Å [4] and $[W_2(\mu\text{-}H)_2(CO)_{10}]^{2-}$ with W–H = 1.926(3) Å [2]. The slighty shorter mean Ir–H bond distance observed here is consistent with iridium's position, to the right of tungsten, rhenium and osmium in the periodic table. The mean Ir–H–Ir bond angle of 87.8(4)° is at the low end of the recorded range (85°–159°); this is consistent with the observed short Ir–Ir bond distance of 2.465(3) Å (electron counting, to satisfy the 18-electron rule, suggests an M≡M triple bond). This angle may be compared to that in $[(PEt_2Ph)_2Re]_2(\mu\text{-}H)_4(H)_4$ which is also presumed to have an M≡M triple bond (again, from electron counting considerations) with Re–Re = 2.538(4) Å, and which exibits an average acute M–H–M bond angle of 85.0(3)°.

The disordered hydride ligands in 1^+ are in an essentially equilateral triangular arrangement in a plane at right angles to the Ir–Ir axis, with H---H non-bonding contact distances of 2.20–2.24(2) Å. Other bond lengths and angles (Table 5) are within the expected normal ranges.

Conclusions

In conclusion, the $[(C_5(CH_3)_5Ir)_2(\mu\text{-}H)_3]^+$ cation has been reexamined by neutron diffraction, this time utilizing a large, high quality crystal of the $[ClO_4]^-$ derivative. The selected crystal diffracted strongly, resulting in a data set which refined to yield a low R factor ($R(F)$ = 0.038). The unusual shapes of the bridging hydride probability ellipsoids (see Fig. 2) have been shown to be due to a hitherto overlooked disorder in the structure, which results in a situation where the three hydrides are seen as six disordered half-occupied hydrogens, with each pair of half-hydrogens clearly resolved. When this disorder is taken into account and the six half-hydrogens are refined isotropically, the final structure model is obtained (see Fig. 3). In spite of the presence of disorder, the R factor and the standard deviations are sufficiently low to consider this a definitive structural analysis, thus filling in the gap in the symmetric M–$(H)_n$–M series, with characterization of compounds now up to and including $n = 4$. The bond distance trend in the series for the third-row metals is W–H(br) = 1.926(3), Re–H(br) = 1.878(8), Os–H(br) = 1.850(5) and Ir–H(br) = 1.78(1) Å. Given the short H–H non-bonding contact (1.870(8) Å) in the $n = 4$ complex, it may not be possible for more than four hydrides to 'fit' around any M–M bond for transition metals [22]. Thus, one may have to turn to larger atoms (the actinides and/or lanthanides) to further expand the M–$(H)_n$–M series.

Supplementary Material

Atomic positional and thermal parameters from the X-ray study (Tables S1 and S2); observed and calculated structure factors (Table S3, X-ray; Table S4, neutron) (30 pages) are available from author R.B.

Acknowledgements

This research was supported by NSF grant CHE 83-20484 (R.B.). Work at Brookhaven National Laboratory was performed under contract DE-ACO2-76CH00016 with the U.S. Department of Energy, Office of Basic Energy Sciences. We would like to thank R. K. McMullan for valuable discussions, D. Rathjen for technical assistance, and E. Abola for his careful review of the manuscript.

References

1 J. P. Olsen, T. F. Koetzle, S. W. Kirtley, M. Andrews, D. L. Tipton and R. Bau, *J. Am. Chem. Soc., 96* (1974) 6621.
2 W. Chiau-Yu, M. W. Marks, R. Bau, S. W. Kirtley, D. E. Bisson, M. E. Henderson and T. F. Koetzle, *Inorg. Chem., 21* (1982) 2556.

3 R. G. Teller, J. H. Williams, T. F. Koetzle, R. R. Burch, R. M. Gavin and E. L. Muetterties, *Inorg. Chem., 20* (1981) 1806.
4 A. G. Orpen, A. V. Rivera, E. G. Bryan, D. Pippard, G. M. Sheldrick and K. D. Rouse, *J. Chem. Soc., Chem. Commun.*, (1978) 723.
5 R. Bau, W. E. Carroll, R. G. Teller and T. F. Koetzle, *J. Am. Chem. Soc., 99* (1977) 3872.
6 R. Bau, W. E. Carroll, D. W. Hart, R. G. Teller and T. F. Koetzle, *Adv. Chem. Ser., 167* (1978) 73.
7 R. G. Teller, *Ph.D. Dissertation*, University of Southern California, 1977.
8 S. C. Abrahams, A. P. Ginsberg, T. F. Koetzle, P. Marsh and C. R. Sprinkle, *Inorg. Chem., 25* (1986) 2500.
9 C. White, A. J. Oliver and P. M. Maitlis, *J. Chem. Soc., Dalton Trans.*, 1901 (1973).
10 J. W. Kang, K. Moseley and P. M. Maitlis, *J. Am. Chem. Soc., 91* (1969) 5970.
11 G. M. Sheldrick, *SHELX Progams*, University of Cambridge, Cambridge, U.K., 1976.
12 D. G. Dimmler, N. Greenlaw, M. A. Kelley, D. W. Potter, S. Rankowitz and F. W. Stubblefield, *IEEE Trans. Nucl. Sci., NS-23* (1976) 298.
13 R. K. McMullan, L. C. Andrews, T. F. Koetzle, F. Reidinger, R. Thomas and G. J. B. Williams, *NEXDAS*, neutron and X-ray data aquisition system, 1976, unpublished work.
14 Air Products and Chemicals, Inc., *Displex Model CS-202.*
15 G. Germain, P. Main and M. M. Woolfson, *Acta Crystallogr., Sect. A, 27* (1971) 368.
16 R. K. McMullan, *Program DIFSYN*, unpublished work.
17 J.-O. Lundgren, Crystallographic computer programs, *Report UUIC-B13-4-05*, Institute of Chemistry, University of Uppsala, Uppsala, Sweden, 1982.
18 P. J. Becker and P. Coppens, *Acta Crystallogr., Sect. A, 31* (1975) 417.
19 L. Koester, in *Neutron Physics*, Springer, Berlin/Heidelberg/New York, 1977, p. 36.
20 P. Coppens, L. L. Leiserowitz and D. Rabinovich, *Acta Crystallogr., 18* (1965) 1035.
21 C. K. Johnson, *Program ORTEP2, Report ORNL-5138*, Oak Ridge National Laboratory, TN, U.S.A., 1976.
22 A. Dedieu, T. A. Albright and R. Hoffmann, *J. Am. Chem. Soc., 101* (1979) 3141.